

# Intramolecular $\pi$ -Stacking in Isostructural Conformational Probes Depends Strongly on Charge Separation, a Proton NMR Study

Pramod Prasad Poudel,<sup>[a]</sup> Jing Chen,<sup>[b]</sup> and Arthur Cammers\*<sup>[a]</sup>

**Keywords:**  $\pi$ -Stacking / Solution state / Crystalline state / Conformation / NMR anisotropy

Our solution state conformational methods used previously to study a dicationic molecular template for intramolecular aromatic association were applied to a neutral hydrocarbon analogue to probe the effect of charge on conformation. Conformational analysis of the hydrocarbon revealed modest solvent dependence in largely unfolded molecules. Conformations found in the solid state were unfolded also corroborating the findings of the solution-state study. This study also adds solid-state evidence for three competing solution-state

conformers previously predicted by calculations. In the absence of charge, the molecular template does not favor intramolecular association of aromatic substituents. These results agree with the chemical literature and previous reports of neutral hydrocarbon intramolecular association in the solution state.

(© Wiley-VCH Verlag GmbH & Co. KGaA, 69451 Weinheim, Germany, 2008)

## Introduction

In an approach encapsulated by the early ideas of Karabatsos,<sup>[1]</sup> and in work by Fukazawa,<sup>[2–7]</sup> and others,<sup>[8–12]</sup> a calculation-based/<sup>1</sup>H NMR-based, multi-state mathematical model for the solution-phase conformation of the dicationic **1a–c** was devised.<sup>[10–12]</sup> The steps involved in these conformational analyses were: 1) molecular modeling and X-ray crystallography to locate candidate conformational energy minima, and grouping these conformations into classes, 2) ab initio calculations of the effect of anisotropy on key chemical shifts in these conformations. Figure 1 displays the calculated anisotropic shielding tensor of benzene with shielding and deshielding regions at the  $\pi$ -face and edge respectively. 3) experimentally measuring the chemical shift difference between key, analogous chemical shifts of the template molecule and an ideal reference molecule, 4) solving a system of equations designed to output the conformational distribution given the computed chemical shifts, the experimental chemical shifts and mass balance, 5) checking the stability of the mathematical model by grouping conformations and omitting the expression for mass balance under different conditions (temperature and solvent) to look for negative concentrations of conformers in the output of the algorithm.

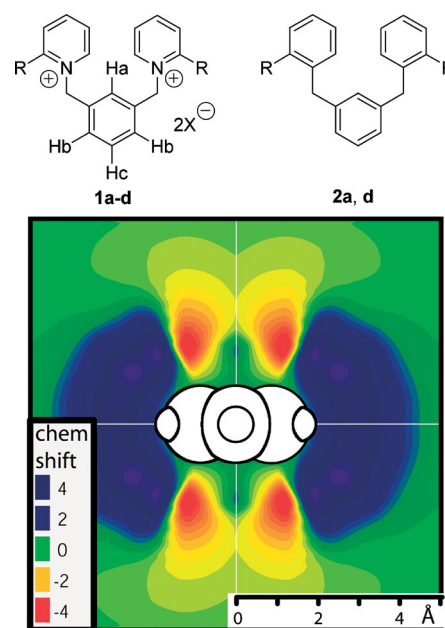


Figure 1. Above: NMR-assayable  $\pi$ -stacking molecular template. **a**: R = Ph; **b**: R = 2,4,6-trifluorophenyl; **c**: R = pentafluorophenyl; **d**: R = methyl. X = Br or PF<sub>6</sub>. Below: The numbers are chemical shifts due to shielding in the vicinity of the benzene ring calculated at rb3lyp/6-311++g(2d,2p) and plotted as a contour slice through C<sub>6</sub>H<sub>6</sub>, shown in CPK. The calculation starts at 2 Å on the x axis and 1.5 Å on the z axis from the benzene centroid.

[a] University of Kentucky, Department of Chemistry, Chemistry-Physics Building, 505 Rose St., Lexington, KY 40506-0055, USA  
Fax: +1-859-323-1069  
E-mail: a.cammers@uky.edu

[b] University of Kentucky, College of Pharmacy, 725 Rose Street, Lexington, KY 40536, USA

Supporting information for this article is available on the WWW under <http://www.eurjoc.org> or from the author.

Molecular modeling and solid-state studies elucidated four conformations that could compete at room temperature. Two unfolded, splayed, **S**, conformational classes and two folded, **C** (3-ring cluster) and **F** ( $\pi$ -face-to-face), conformational classes had different NMR signatures due to the

anisotropy of the phenyl rings attached to the pyridinium moiety.<sup>[13,14]</sup> In the development of this conformational analysis **1b–c** were important,<sup>[13]</sup> but these molecules are not considered here in any detail. The current study aims to validate previous conformational studies, and aims to investigate the condition-dependent conformation of **2a**.

## Results and Discussion

### Methods

The effects of anisotropic shielding on the chemical shifts of microstates comprising conformations **C**, **F** and **S** were calculated by ab initio methods. Experimental differences between the chemical shifts of **1a** and **1d** of the three analogous, symmetry-independent protons of the xylene moiety were used in simultaneous equations. The same model was used with **2a** and **2d**. Solving these equations gave the distributions of the conformational classes **C**, **F** and **S** of **1a–c** under various conditions.<sup>[13–15]</sup> Compound **1d** was approximated to have no connection between conformational changes and chemical shift. We estimated that **1d** corrected the drift in chemical shifts of Ha–Hc due to bulk solvent effects and due to changes in ion pairing. Protons Ha and Hb of the phenylated material had more magnetic dispersion and more variable chemical shifts than the methylated reference compounds. However, the variability in the chemical shift of Hc was similar in **1a** and **1d**. Greater appreciation for this can be seen graphically in the Supporting Information section entitled: *Relative Chemical Shift of Ha vs. Hc as a Function of Solvent Dielectric*.

One conformational class, **C**, found by molecular modeling<sup>[13]</sup> (the global minimum) formed a three-ring aromatic cluster, which pushed the methine signal of Ha upfield relative to Hb. The **C** state allowed three rings to cluster, an aspect of gas and solution phase aromatic interactions.<sup>[16,17]</sup> The **C** state also accounted for the previous observation that three phenyl rings gave much evidence for folded conformation but two phenyl rings gave little.<sup>[18,19]</sup> Conformational class, **F**, maintained a  $\pi$ -face-to-face relationship between the xylyl and the phenyl rings, but induced upfield shifts at Ha and Hb nearly equally. A structural average of three microstates modeled the **F** state: one microstate put the phenyl ring above Ha, another put phenyl above Hb. Figure 2, structure **F**, from computational conformation searching, shows these two conformational contributions with phenyl proximal to Ha (above) and the other near Hb (below). The third conformational contribution to the **F** state put the phenyl ring with respect to Hb in a spatially identical manner as the **C** state with respect to Ha. The magnetic effects of these three conformers were averaged to compose the **F** state because calculations indicated that there were minimal energetic differences between them.

Two splayed (unfolded) conformations derived from two low-energy biaryl dihedral angles were found by molecular modeling. **SeF** or **See** signify an edge-to-face or an edge-to-edge spatial relationship between phenyl and xylyl. Whether

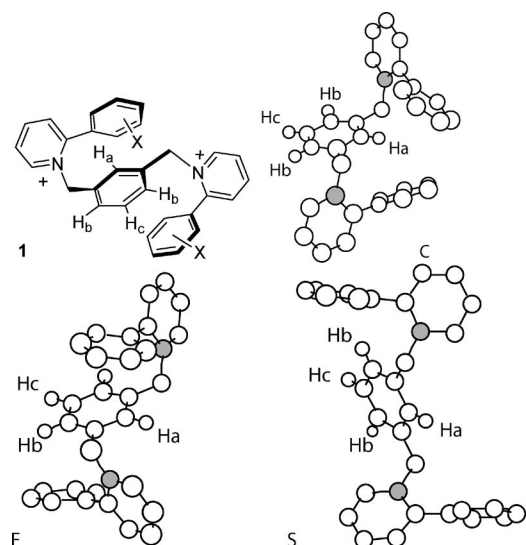


Figure 2. Components in an NMR-based solution-state conformational analysis of **1**.

the phenyl is proximal to Ha (**S** in Figure 2 is **SeF**, lower right) or proximal to Hb (structure **S** in Figure 2, upper left) produces two related conformational classes, each composed of two microstates.

The conformational analysis took advantage of the fact that **1** and **2** have dynamic  $C_{2v}$  symmetry; the chemical shifts of half structures were calculated. To calculate and map the chemical shift anisotropy of the phenyl substituents on xylyl Ha–Hc in all the conformational microstates, the model was further simplified. The xylyl ring was erased and  $H_2$  molecules replaced the xylyl C–H bonds at Ha–Hc. The 2-phenylpyridinium moiety was replaced with fluorobenzene. NMR chemical shift calculations were performed on these simple systems to estimate the magnetic shielding of the aromatic ring. Equations 1–4 were used to determine the mol fractions of the conformers present in solution with chemical shift as the independent variable.<sup>[15]</sup>

$$X_C + X_F + X_{See} + X_{SeF} = 1 \quad (1)$$

$$\delta 1d(Ha) - \delta 1a(Ha) = 2C_a X_C + 2F_a X_F + 2See_a X_{See} + 2SeF_a X_{SeF} \quad (2)$$

$$\delta 1d(Hb) - \delta 1a(Hb) = C_b X_C + F_b X_F + See_b X_{See} + SeF_b X_{SeF} \quad (3)$$

$$\delta 1d(Hc) - \delta 1a(Hc) = 2C_c X_C + 2F_c X_F + 2See_c X_{See} + 2SeF_c X_{SeF} \quad (4)$$

Equation (1) is an expression of mass balance; the X values are mol fractions of the conformational classes described above, dependent variables to be determined by the solution of these four equations. Equations 2–4 express differences in chemical shift between **1d** and **1a** at Ha, Hb and Hc, respectively. For **2a**, **2d** was used as the reference. In the equations,  $C_a$ ,  $F_a$  or  $See_a$  etc. are calculated constants of proportionality relating chemical shift differences [e.g.  $\delta 1d(Ha) - \delta 1a(Ha)$ ] to mol fraction. These coefficients appear in Table 1. Because two phenyl rings can affect Ha and Hc simultaneously, their corresponding coefficients are

multiplied by 2 in Equations 2 and 4. Equation (3) does not take this form because there are two symmetrically equivalent Hb protons which share the effects of the two phenyl rings.

Table 1. Values of the coefficients used in the equations above.

Coefficient <sup>[a]</sup>	Ha	Hb	Hc
<b>C</b>	1.70	0.19	0.07
<b>F</b>	0.52	1.26	0.40
<b>See</b>	-0.80	-0.67	0.13
<b>Sef</b>	0.14	0.22	0.00

[a] Coefficients were calculated at the rb3lyp/6-311++g(2d,2p) level.

The model is not perfect. One approximation in the model is the way that the **F** states and the **S** states are binned to comprise the distribution. Better math would tell us if the phenyl prefers the Ha or the Hb side of the ring in the **S** states for example. However there is not enough information in the spectra for this level of analysis. Another approximation in this conformational analysis labels **S** states unfolded and **C** and **F** states folded; there is perhaps some residual intramolecular aryl-aryl contact in the **S** states. An analysis of the solvent accessible surface area of the conformations was presented previously as an argument for classifying the conformations in this manner.<sup>[14]</sup> Calculations in the gas phase overestimate the effect of chemical shift anisotropy when distances allow solvent to fit between the phenyl ring and the proton of interest. In the mathematical model these go from small to zero to correct for shielding by solvent (coefficient for **Sef**, Hc in Table 1).<sup>[15]</sup>

Preoccupation about these issues instigated checks of Equations 2–4 for molecules **1a–c** by averaging the **S** state expressions and excluding the hard-wired mass balance of Equation (1); the mass balanced in these systems of equations within ca. 10%. Descriptions of these checks are available in greater detail.<sup>[15]</sup>

The mathematical model that connected experimental chemical shift differences to the conformation of **1a** should perform as well for **2a** once the ideal chemical shift reference is changed to **2d**. Successful application requires near equivalent NMR anisotropy of monosubstituted phenyl rings so that the substituents: *N*-xylylpyridinium-2-yl of **1a**, 2-xylylphen-1-yl of **2a** and the F atom substituent in the model exert similar magnetic effects on the chemical shifts of proximal atoms. This was found not to be the case for **1a**, **1b** and **1c**. The constants in Equations 2–4 had to be calculated for each of these separately.<sup>[15]</sup>

To probe the applicability of the chemical shift constants used for **1a** to the conformational analysis of **2a**, chemical shift calculations of a series of monosubstituted benzene rings that spanned the usual linear free energy relationship were run and the results were plotted against sigma-para.<sup>[20,21]</sup> An H atom in H<sub>2</sub> was put at (*x*, *y*, *z*: 0.49, 0.49, 2.6 Å) with respect to a phenyl ring positioned with C1, and C4 along the horizontal axis; all C atoms were in the *xy* plane and the phenyl centroid was at 0, 0, 0. The results are summarized in Figure 3. There are three points for phenyl because the most popular biphenyl dihedrals were

tried. The probe H<sub>2</sub> molecule placed at the phenyl perimeter produced similar muted effects. Figure 3 shows that the chemical shift is more dependent on mono-substitution than on the nature of the substituent. Thus, differences between **1a** and **2a** should be corrected by the NMR references **1d** and **2d** respectively.

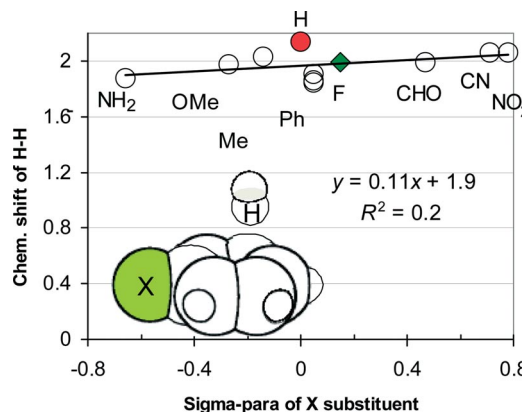


Figure 3. The effect of anisotropy on the chemical shift of H<sub>2</sub> at H as a function of  $\sigma$ -para of X. In this study the fluoro substituent ( $\diamond$ ) modeled monosubstitution. The benzene ring (O) deviated the most from the trend. Low  $R_2$  indicates poor linear relationship.

### Solid State

The crystallographic information files (CIF) are available as supplementary data. Previous studies<sup>[13–15]</sup> only presented solid-state evidence for the **F** state with the phenyl ring positioned proximal to Ha in the dibromide salts of **1a–c**. The other conformational microstates comprising conformations **C**, **F** and **S** represented low-energy states from calculations: conformational searches with Amber\* as implemented in Macromodel.<sup>[22]</sup> The crystal structure (Figure 4, middle) of the **1a**-2PF<sub>6</sub> salt belongs to the **F** conformational group with the phenyl rings above Hb. This conformational microstate was previously used to construct the mathematical model of the **F** state, but was only supported on the basis of calculation. The carbon atom and nitrogen atomic positions of the solid state of **1a**-2PF<sub>6</sub> and the **F** state with the phenyl over Hb used previously overlapped with a root mean square (RMS) difference of 0.2 Å. These calculations are described further in the Supporting Information under the heading *root mean square positional similarity*.

Solid state evidence that **1** and **2** model  $\pi$ -stacking comes from the fact that the di-PF<sub>6</sub> methyl derivative **1d**-2PF<sub>6</sub> crystallized in an **S** state (not shown). If it were phenyl and not methyl, the phenyl rings in this conformation would not intramolecularly associate with the xylyl ring. These two crystal structures (**1a**-2PF<sub>6</sub> and **1d**-2PF<sub>6</sub>) in the absence of other data might have led one tentatively to the hypothesis that the phenyl rings provide the cohesive force to favor the folded states.

Another switch in solid-state conformation occurred when the N atoms in **1a** were substituted with C atoms to produce the neutral all hydrocarbon derivative **2a**. Inspec-

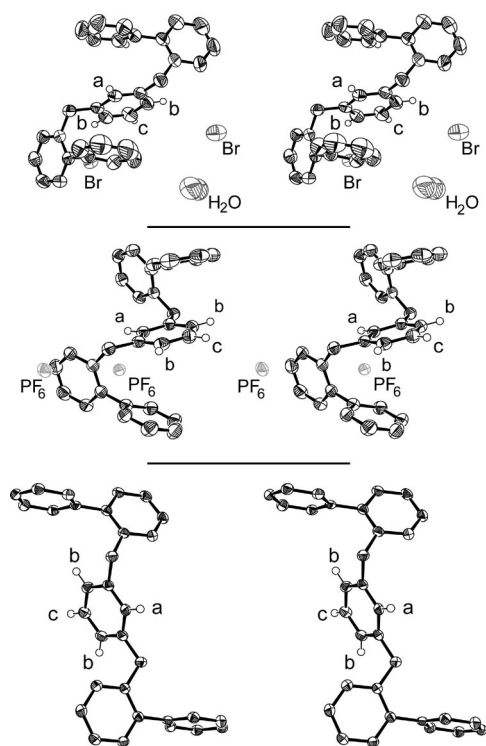


Figure 4. ORTEP stereoviews of X-ray structures of **1a** 2Br + H<sub>2</sub>O, **1a** 2PF<sub>6</sub>, F atoms not shown, and **2a**.

tion of the crystal structure of **2a** revealed a conformer that possessed two symmetry-unrelated S conformations at either end of the molecule. To quantify how closely the solid state of **2a** resembled any of the four microstates used to model the magnetic behavior of the S conformation in the previous analyses of **1**, RMS differences in analogous atomic positions were calculated between the two ends of the solid state conformer of **2a** and the previously calculated S states of **1a**. These RMS differences were compared to RMS differences in atomic coordinates between the solid state of **2a** and previous C and F states of **1**. The atomic coordinates of the conformer in the solid state of **2a** overlapped well with two S states used previously. The description of this analysis is available in the Supporting Information under the heading *Root Mean Square Atomic Positional Similarity*.

### Solution State

Figure 5 graphically shows the solvent dependence of the conformations of **1a**-2PF<sub>6</sub>, **1a**-2Br and neutral **2a** from simultaneous solutions of Equations 1–4 with NMR chemical shifts of Ha, Hb and Hc as input. Missing points are due to insolubility. Grossly, the conformations in the molecules change as a function of solvent dielectric although one would expect microscopic solvent properties to be influential. These microscopic effects might be manifest in the solvent-dependent mol fraction in the four curves at point 7, CD<sub>3</sub>CN. However, microscopic solvent effects are beyond the current analysis.

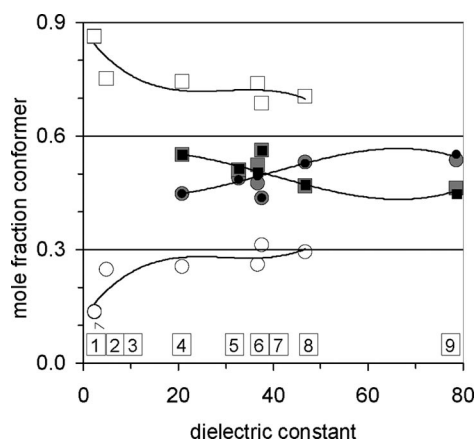


Figure 5. The mol fraction folded (F+C) [circles] and unfolded S [squares] are plotted as a function of solvent dielectric for **1a**-2PF<sub>6</sub> [grey], **1a**-2Br [black] and **2a** [white]. Solvents: (1) C<sub>6</sub>D<sub>6</sub> (2) [D<sub>8</sub>]Tol (3) CDCl<sub>3</sub> (4) [D<sub>6</sub>]acetone (5) CD<sub>3</sub>OD (6) [D<sub>7</sub>]DMF (7) CD<sub>3</sub>CN (8) [D<sub>6</sub>]DMSO (9) D<sub>2</sub>O.

From the solvent-dependent conformation of **1a** and **2a** in Figure 5 the initial purpose of this study was fulfilled. Molecule **2a** and **2d** were synthesized to test **1a** as a model for  $\pi$ -stacking. If the conformations of **2a** had not changed with the solvent in a similar manner to **1a** we would have to ascribe something other than the native attraction of the rings to one another as the major factor in control of conformation. Figure 5 shows that increasing solvent polarity tends to fold both molecules and the trend appears to be modestly solvophobic.<sup>[23]</sup> The conformational aspects of both molecules being a function of  $\pi$ -stacking, as stated above, was corroborated by the fact that **1a**-2PF<sub>6</sub> crystallized in an F conformation and **1d**-2PF<sub>6</sub> crystallized in a splayed open conformation. The fact that **1a**-2Br and **1a**-2PF<sub>6</sub> behave similarly also corroborates the notion that intramolecular interactions in the cation and changes in solvent contact govern conformation. This justifies the original control experiments for this issue which compared the conformational behavior of **1a**-2Br to **1a**-2Cl.<sup>[13]</sup>

The other salient feature of the graph in Figure 5 is that neutral **2a** is less folded than charged **1a**. This result agrees with the conformations found in the solid states in that **1a**-2PF<sub>6</sub> and **1a**-c-2Br crystallized in two distinct F conformations from polar solvent, but **2a** crystallized in a mixed S conformation from a non-polar solvent mixture (10:1 hexane/EtOAc) in which the fraction unfolded conformation was likely ca. 90%.

In the previous study of this system **1b** and **1c** progressively promoted unfolding.<sup>[15]</sup> The disposition of the aromatic rings in the general structure of **1a** promote face-to-face, edge-to-center association between the xylyl and phenyl rings.<sup>[18,24]</sup> Putative quadrupolar enhancement of aromatic association by progressive substitution with F atoms would depend on a face-to-face, center-to-center association.<sup>[25,26]</sup> However, such an interaction is inhibited by torsional strain in the general structure of **1** and **2**. In the current study, N-to-C substitution promoted unfolding of similar magnitude to that observed for **1c** with the caveat

that **1c-2Br** did not unfold to the extent that **2a** unfolded due to limitations in solubility with nonpolar solvents.

The conformational behavior of the all-carbon analogue brings our  $\pi$ -stacking model in line with previous reports in the chemical literature. Even though solvent is an important factor in the global conformation of biological polymers due to synergism in many modest interactions toward a native state, generally solvent-sensitive conformation in small organic molecules is rare and not very dramatic.<sup>[27,28]</sup> When observed, solvent-dependent conformation relies on strong interactions between dipoles or changes in the solvent's ability to hydrogen bond with a group upon conformational change.

The chemical literature indicates that **1a** should favor folded conformations and **2a** should not. Studies of derivatives of monocation half structures of **1a** indicate that electrostatic effects increase the rotational barrier of the C–N bond.<sup>[24]</sup> In studies of a wide variety of template molecules (Figure 6) aimed toward the measurement of intramolecular aromatic interactions,<sup>[26,29]</sup> more favorable interactions were found when at least one electron-poor aromatic group was involved.<sup>[26]</sup> Favorable interactions were not detected or interactions were found to be repulsive between electron-rich, or between all hydrocarbon, aromatic rings (**3** and **4**).<sup>[9,30–32]</sup> In Wilcox' ingenious template **5**, the aromatic interactions were not as cohesive as the alkyl/aromatic interactions.<sup>[33]</sup> Other studies show that aromatic hydrocarbon interactions are very weak even when structural analysis puts these groups within interaction distances, **6**<sup>[8,34,35]</sup> com-

pared to heteroatom analogues.<sup>[36–39]</sup> The aromatic interactions increase when substituents perturb the electronic nature of the rings.<sup>[40,41]</sup>

Incisive calculations of intermolecular interactions of small arene derivatives gave similar dependences on the electronic nature of aryl substituents.<sup>[42,43]</sup> In related studies of intermolecular aromatic association in large  $\pi$ -systems, again, one or more electron-deficient aromatic component exalts cohesion at the molecular level.<sup>[44–47]</sup> When at least one component in the aromatic interactions is electron-poor, attractions between aromatic groups neatly explain synthetic<sup>[48–50]</sup> and computational results.<sup>[51]</sup> As assayed by many solution-phase methods, neutral hydrocarbon aromatic interactions have been found to be very weak; they are certainly weak relative to the amount of attention that they routinely receive in the chemical literature. By default, in the chemical literature  $\pi$ -stacking more often than not refers to cohesive forces based on weak electrostatic interactions instead of the canonical dispersive interaction between aromatic moieties; however, the latter is the usual mental picture invoked by  $\pi$ -stacking.

## Conclusions

While the conformation of the solid state might not generally be assumed to be the preferred conformation in the solution state, this study found the preferred conformations in solution and in the solid state to be similar. The three *ortho*-aryl derivatives, **1a–c**, crystallized in folded, stacked conformations and favored the folded solution state, whereas **2a** crystallized in an unfolded conformation and was found to prefer an unfolded conformational state in solution.

Previous conclusions that interactions between the aryl substituents folded this molecular family were corroborated by the current study in that the conformational effects were found to be governed by the very modest attraction between aromatic groups. Consonant with other reports in the chemical literature, interactions between hydrocarbon aromatic groups of organic molecules in solution phase are unremarkable in the control of conformation. This report is the sixth and most likely the last of our studies of the conformation of this molecular family.

## Experimental Section

**General:** Melting points are uncorrected. Solid-state data on all the compounds were collected with a Nonius kappaCCD diffractometer; cell refinement and data reduction were done using SCALEPACK and DENZO-SMN.<sup>[52]</sup> Structure solution and refinement were carried out using the SHELXS97 and SHELXL97 program, respectively.<sup>[53]</sup>

CCDC-697018 (for **1a-2PF<sub>6</sub>**), -697019 (for **1d-2PF<sub>6</sub>**) and -697020 (for **2a**) contain the supplementary crystallographic data for this paper. These data can be obtained free of charge from The Cambridge Crystallographic Data Centre via [www.ccdc.cam.ac.uk/data\\_request/cif](http://www.ccdc.cam.ac.uk/data_request/cif).

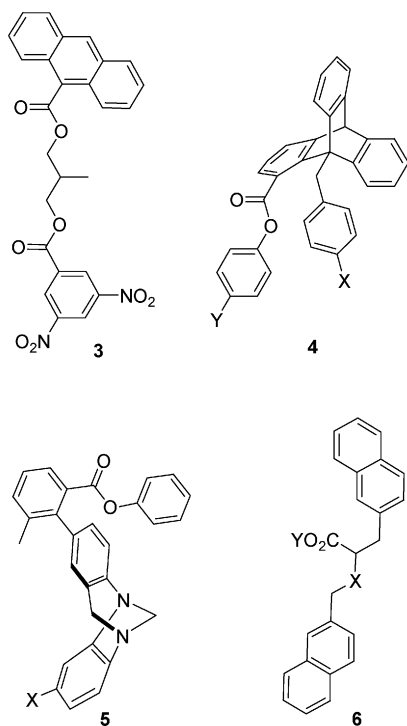


Figure 6. Some conformational templates of aromatic interactions in the chemical literature.

**<sup>1</sup>H NMR Studies:** Conformation of **1a** and **2a** were studied using two NMR tubes; one tube contained the phenyl analog and the other contained the reference compound **1d** or **2d** in the identical solvent. Temperature-controlled measurements were recorded to three digits past the decimal after the lack of drift in chemical shifts indicated thermal equilibrium. See previous studies for more details.<sup>[14,15]</sup>

**Synthesis:** Counter ion exchange to synthesize **1a-2PF<sub>6</sub>** and **1d-2PF<sub>6</sub>**, X-ray diffraction analysis of the crystals thus obtained confirmed atomic connectivity and hexafluorophosphate ions. *α,α'*-*m*-xylylene-*N,N'*-bis(2-phenylpyridinium) dihexafluorophosphate (**1a-2PF<sub>6</sub>**): To a solution of *α,α'*-*m*-xylylene-*N,N'*-bis(2-phenylpyridinium) dibromide,<sup>[13]</sup> **1a-2Br** (66 mg, 0.115 mmol) in water (20 mL) was added ammonium hexafluorophosphate (50 mg, 0.307 mmol). A white precipitate formed immediately which dissolved upon heating under N<sub>2</sub>. Slow cooling of the solution to room temperature gave white needle-like crystals of **1a-2PF<sub>6</sub>** (73.4 mg, 91% yield); dec. 219–221 °C. <sup>1</sup>H NMR spectroscopic data in D<sub>2</sub>O were indistinguishable from the published spectrum of **1a-2Br**. X-ray diffraction analysis of the crystal thus obtained confirmed atomic connectivity and hexafluorophosphate ions. *α,α'*-*m*-xylylene-*N,N'*-bis(2-methylpyridinium) dihexafluorophosphate (**1d-2PF<sub>6</sub>**): The same method above using *α,α'*-*m*-xylylene-*N,N'*-bis(2-methylpyridinium) dibromide,<sup>[13]</sup> **1d-2Br** with 100 mg, 0.222 mmol gave **1d-2PF<sub>6</sub>** as a colorless crystal upon slow evaporation of water from an open tube (110 mg, 85% yield), 188–190 °C, decomp. <sup>1</sup>H NMR spectrum in D<sub>2</sub>O was ca. indistinguishable from the published <sup>1</sup>H spectrum of **1d-2Br**.<sup>[13]</sup>

**1,3-Bis(biphenyl-2-yl)methylbenzene (2a):** Reactions were performed under N<sub>2</sub>. An oven-dried, 50 mL flask, fitted with a condenser was charged with *α,α'*-dibromo-*m*-xylene (394.5 mg, 1.5 mmol), Pd(PPh<sub>3</sub>)<sub>4</sub> (115.5 mg, 0.1 mmol), and 20 mL 1,2-dimethoxyethane (DME). The bright yellow solution was stirred at room temperature for 20 min. Sequential addition of 2-biphenylboronic acid (682.4 mg, 3.45 mmol), *t*BuOK (672 mg, 6.0 mmol), *t*BuOH (3.0 mL) and Ag<sub>2</sub>O<sup>[54]</sup> (1.4 g, 6.0 mmol) resulted in a dark solution and the formation of a dark precipitate. The mixture was refluxed under nitrogen at 85 °C for 17 h. The mixture was cooled, concentrated in vacuo, and partitioned between EtOAc/H<sub>2</sub>O (1:1, 120 mL). The layers were separated and the aqueous layer was washed with two additional 60 mL portions of EtOAc. The combined organic layers were dried with MgSO<sub>4</sub> and concentrated in vacuo. Silica gel column chromatography (hexane/CHCl<sub>3</sub>, 4:1) gave **2a** as a colorless solid that crystallized from 10:1 hexane/EtOAc (190 mg, 31%); m.p. 132–134 °C. <sup>1</sup>H NMR (400 MHz, CDCl<sub>3</sub>): δ = 7.30 (m, 12 H), 7.19 (m, 6 H), 7.07 (t, *J* = 7.6 Hz, 1 H), 6.79 (d, *J* = 7.6 Hz, 2 H), 6.59 (s, 1 H), 3.87 (s, 4 H) ppm. <sup>13</sup>C NMR (100 MHz, CDCl<sub>3</sub>): δ = 142.4, 141.8, 141.5, 138.5, 130.5, 130.3, 129.8, 129.5, 128.3, 128.2, 127.6, 127.0, 126.5, 126.3, 39.2 ppm. MS (IE): *m/z* = 410 (38) [M], 411 (34/35 (calcd.)) [M + 1], 412 (6) [M + 2], 243 (31) [M – (2-methylbiphenyl)], 244 (21) [M – (2-methylbiphenyl) + 1]. X-ray diffraction confirmed the atom connectivities.

**1,3-Bis(2-methylphen-1-yl)methylbenzene (2d):** The above method with *o*-tolylboronic acid (469.2 mg, 3.45 mmol) after silica gel column chromatography (hexane/CHCl<sub>3</sub>, 3:1) gave **2d** as white solid; m.p. 36–38 °C (176 mg, 41%). <sup>1</sup>H NMR (400 MHz, DMSO): δ = 7.14 (t, *J* = 7.6 Hz, 1 H), 7.07 (m, 8 H), 6.93 (s, 1 H), 6.90 (d, *J* = 7.6 Hz, 2 H), 3.87 (s, 4 H), 2.13 (s, 6 H) ppm. <sup>13</sup>C NMR (100 MHz, CDCl<sub>3</sub>): δ = 140.9, 139.7, 136.7, 130.7, 130.2, 129.7, 129.0, 126.9, 126.8, 126.5, 39.2, 19.9 ppm. MS (IE): *m/z* = 286 (79) [M], 287 (24) [M + 1], 181 (100) [M – xylyl], 182 (15) [M – xylyl + 1].

**Supporting Information** (see also the footnote on the first page of this article): Tables 2–4 report the measured <sup>1</sup>H NMR chemical

shifts of **1a-2Br**, **1d-2Br**, **1a-2PF<sub>6</sub>**, **1d-2PF<sub>6</sub>**, **2a** and **2d** in the solvents used in Figure 5. Graphs comparing the conditional chemical shifts of **1a**, **2a**, **1d** and **2d**. RMS differences in the comparison of the solid state of **2a** and the conformations used previously, demonstrating that the solid state of **2a** is an S state. Sample <sup>13</sup>C and <sup>1</sup>H NMR spectra are available for **2a** and **2d**.

## Acknowledgments

The authors thank the National Science Foundation USA (# 0111578) for funding this research; we are also grateful to the University of Kentucky's Center for Computational Sciences.

- [1] G. J. Karabatsos, D. J. Fenoglio in *Rotational Isomerism about sp<sup>2</sup>–sp<sup>3</sup> Carbon-Carbon Single Bonds*, vol. 5 (Eds.: E. L. Eliel, N. L. Allinger), Wiley Interscience, New York, 1970, pp. 167–203.
- [2] Y. Fukazawa, S. Usui, K. Tanimoto, Y. Hirai, *J. Am. Chem. Soc.* 1994, 116, 8169–8175.
- [3] Y. Fukazawa, T. Hayashibara, Y. Yang, S. Usui, *Tetrahedron Lett.* 1995, 36, 3349–3352.
- [4] H. Iwamoto, Y. Yang, S. Usui, Y. Fukazawa, *Tetrahedron Lett.* 2001, 42, 49.
- [5] Y. Fukazawa, T. Haino, Y. Kondoh, *Tetrahedron Lett.* 1999, 40, 3591–3594.
- [6] Y. Fukazawa, S. Usui, *J. Synth. Org. Chem. Jpn.* 1997, 55, 1124–1133.
- [7] Y. Fukazawa, S. Usui, K. Ogata, *J. Am. Chem. Soc.* 1988, 110, 8692–8693.
- [8] L. F. Newcomb, T. S. Haque, S. H. Gellman, *J. Am. Chem. Soc.* 1995, 117, 6509–6519.
- [9] N. J. Heaton, P. Bello, B. Herradon, A. del Campo, J. Jimenez-Barbero, *J. Am. Chem. Soc.* 1998, 120, 12371–12384.
- [10] S. Klod, E. Kleinpeter, *J. Chem. Soc. Perkin Trans. 2* 2001, 1893–1898.
- [11] N. H. Martin, N. W. Allen, K. D. Moore, L. Vo, *THEOCHEM* 1998, 454, 161–166.
- [12] I. Alkorta, J. Elguero, *New J. Chem.* 1998, 22, 381–385.
- [13] H. R. Mulla, A. Cammers-Goodwin, *J. Am. Chem. Soc.* 2000, 122, 738–739.
- [14] M. D. Sindkhedkar, H. R. Mulla, A. Cammers-Goodwin, *J. Am. Chem. Soc.* 2000, 122, 9271–9277.
- [15] J. Chen, A. Cammers-Goodwin, *Eur. J. Org. Chem.* 2003, 3861–3867.
- [16] T. Morimoto, H. Uno, H. Furuta, *Angew. Chem. Int. Ed.* 2007, 46, 3672–3675.
- [17] M. O. Sinnokrot, C. D. Sherrill, *J. Phys. Chem. A* 2006, 110, 10656–10668.
- [18] C. B. Martin, H. R. Mulla, P. G. Willis, R. Cammers-Goodwin, *J. Org. Chem.* 1999, 64, 7802–7806.
- [19] C. B. Martin, B. O. Patrick, A. Cammers-Goodwin, *J. Org. Chem.* 1999, 64, 7807–7812.
- [20] E. V. Anslyn, D. A. Dougherty, *Modern Physical Organic Chemistry*, University Science Books, Sausalito, CA, 2006.
- [21] N. Isaacs, *Physical Organic Chemistry*, Pearson/Pentice Hall, Harlow, England, 1995.
- [22] F. Mohamadi, N. G. J. Richards, W. C. Guida, R. Liskamp, M. Lipton, C. Caufield, G. Chang, T. Hendrickson, W. C. Still, *J. Comput. Chem.* 1990, 11, 440–467.
- [23] R. R. Gardner, S. L. McKay, S. H. Gellman, *Org. Lett.* 2000, 2, 2335–2338.
- [24] M. J. Rashkin, M. L. Waters, *J. Am. Chem. Soc.* 2002, 124, 1860–1861.
- [25] J. H. Williams, *Acc. Chem. Res.* 1993, 26, 593–598.
- [26] C. A. Hunter, K. R. Lawson, J. Perkins, C. J. Urch, *J. Chem. Soc. Perkin Trans. 2* 2001, 651–669.
- [27] C. L. Perrin, M. A. Babian, I. A. Rivero, *J. Am. Chem. Soc.* 1998, 120, 1044.

- [28] B. Bhayana, C. S. Wilcox, *Angew. Chem. Int. Ed.* **2007**, *46*, 6833–6836.
- [29] W. B. Jennings, B. M. Farrell, J. F. Malone, *Acc. Chem. Res.* **2001**, *34*, 885–894.
- [30] B. W. Gung, X. W. Xue, H. J. Reich, *J. Org. Chem.* **2005**, *70*, 3641–3644.
- [31] B. W. Gung, X. W. Xue, Y. Zou, *J. Org. Chem.* **2007**, *72*, 2469–2475.
- [32] P. Bello, N. J. Heaton, A. Chana, J. Jimenez-Barbero, E. Riande, B. Herradon, *J. Phys. Org. Chem.* **2004**, *17*, 71–82.
- [33] E. I. Kim, S. Paliwal, C. S. Wilcox, *J. Am. Chem. Soc.* **1998**, *120*, 11192–11193.
- [34] S. H. Gellman, T. S. Haque, L. F. Newcomb, *Biophys. J.* **1996**, *71*, 3523–3526.
- [35] L. F. Newcomb, S. H. Gellman, *J. Am. Chem. Soc.* **1994**, *116*, 4993–4994.
- [36] K. Avasthi, D. S. Rawat, T. Chandra, D. S. Bhakuni, *Ind. J. Chem.* **1998**, 754.
- [37] K. Avasthia, S. Aswala, R. Kumarb, U. Yadavb, D. S. Rawata, P. R. Maulikb, *J. Mol. Struct.* **2005**, *750*, 179–185.
- [38] K. Avasthia, S. M. Farooqa, S. Aswala, R. Raghunandanb, P. R. Maulik, *J. Mol. Struct.* **2007**, *827*, 88–94.
- [39] T. Itahara, K. Imaizumi, *J. Phys. Chem. B* **2007**, *111*, 2025–2032.
- [40] S. L. Cockroft, C. A. Hunter, *Chem. Commun.* **2006**, 3806–3808.
- [41] F. Hof, D. M. Scofield, W. B. Schweizer, F. Diederich, *Angew. Chem. Int. Ed.* **2004**, *43*, 5056–5059.
- [42] S. Bega, K. Waggonera, Y. Ahmada, M. Watta, M. Lewis, *Chem. Phys. Lett.* **2008**, *455*, 98–102.
- [43] A. L. Ringer, M. O. Sinnokrot, R. P. Lively, C. D. Sherrill, *Chem. Eur. J.* **2006**, *12*, 3821–3828.
- [44] A. S. Shetty, J. Zhang, J. S. Moore, *J. Am. Chem. Soc.* **1996**, *118*, 1019–1027.
- [45] S. L. Cockroft, J. Perkins, C. Zonta, H. Adams, S. E. Spey, C. M. R. Low, J. G. Vinter, K. R. Lawson, C. J. Urch, C. A. Hunter, *Org. Biomol. Chem.* **2007**, *5*, 1062–1080.
- [46] S. L. Cockroft, C. A. Hunter, K. R. Lawson, J. Perkins, C. J. Urch, *J. Am. Chem. Soc.* **2005**, *127*, 8594–8595.
- [47] T. Schaller, U. P. Büchele, F.-G. Klärner, D. Bläser, R. Boese, S. P. Brown, H. W. Spiess, F. Koziol, J. Kussmann, C. Ochsenfeld, *J. Am. Chem. Soc.* **2007**, *129*, 1293–1303.
- [48] M. J. Marsella, Z. Q. Wang, R. J. Reid, K. Yoon, *Org. Lett.* **2001**, *3*, 885–887.
- [49] G. W. Coates, A. R. Dunn, L. M. Henling, J. W. Ziller, E. B. Lobkovsky, R. H. Grubbs, *J. Am. Chem. Soc.* **1998**, *120*, 3641–3649.
- [50] G. W. Coates, A. R. Dunn, L. M. Henling, D. A. Dougherty, R. H. Grubbs, *Angew. Chem.* **1997**, *36*, 248–251.
- [51] B. W. Gung, J. C. Amicangelo, *J. Org. Chem.* **2006**, *71*, 9261–9270.
- [52] Z. Otwinowski, W. Minor in *Processing of X-ray diffraction data collected in oscillation mode*, vol. 276 (Eds.: C. W. J. Carter, R. M. Sweet), Academic Press, San Diego, CA, **1997**, pp. 307–326.
- [53] G. M. Sheldrick, *SHELX97 – Programs for Crystal Structure Solution and Refinement*, **1997**, University of Göttingen, Germany.
- [54] J. Chen, A. Cammers-Goodwin, *Tetrahedron Lett.* **2003**, *44*, 1503–1506.

Received: July 4, 2008  
Published Online: August 28, 2008